Proceedings of AJTEC2011
ASME/JSME 8th Thermal Engineering Joint Conference
March 13-17, 2011, Honolulu, Hawaii, USA

AJTEC2011-44552

LAMINAR NATURAL CONVECTION FROM ISOTHERMAL VERTICAL CYLINDERS: A REVISIT TO A CLASSICAL SUBJECT

Jerod C. Day
Mechanical and Energy Engineering
University of North Texas
Denton, TX USA
Email: jerodday@my.unt.edu

Matthew J. Traum
Mechanical and Energy Engineering
University of North Texas
Denton, TX USA
Email: mtraum@unt.edu

Sandra K. S. Boetcher
Mechanical and Energy Engineering
University of North Texas
Denton, TX USA
Email: sandra.boetcher@unt.edu

ABSTRACT

Laminar natural convection heat transfer from the vertical surface of a cylinder is a classical subject, which has been studied extensively. Furthermore, this subject has generated some recent interest in the literature. In the present investigation, numerical experiments were performed to determine average Nusselt numbers for isothermal vertical cylinders ($10^3 < Ra_L < 10^9$, $0.5 < L/D < 10$, and $Pr = 0.7$) situated on an adiabatic surface in a quiescent ambient environment which will allow for plume growth. Results will be compared with commonly used correlations and a new average Nusselt number correlation will be presented. Furthermore, the limit for which the heat transfer results for a vertical flat plate may be used as an approximation for the heat transfer from a vertical cylinder will be investigated.

NOMENCLATURE

A	coefficient
a	coefficient
AR	aspect ratio, L/D
b	coefficient
c	coefficient
c_p	specific heat at constant pressure
D	diameter of the cylinder
F	function
G	function
g	gravitational constant
Gr_L	Grashof number, $g\beta(T_{cylinder}-T_\infty)D^3/\nu^2$
H	height of solution domain
$\bar{h}$	average heat transfer coefficient
k	thermal conductivity
L	height of cylinder
n	coefficient
Nu_L	average Nusselt number, $\bar{h}D/k$
$Nu_{L,fp}$	average Nusselt number of flat plate
P	dimensionless pressure, $(P-P_\infty)/\rho(\nu D)^2$
p	pressure
p_∞	free-stream pressure
Pr	Prandtl number, $c_p\mu/k$
R,Z	dimensionless cylindrical coordinates, (r,z)/D
r,z	cylindrical coordinates
Ra_L	Rayleigh number, $Gr_L Pr$
T	temperature
$T_{cylinder}$	temperature at the vertical surface of the cylinder
T_∞	temperature of the ambient environment
U_R,U_Z	dimensionless velocity components, $(u_r,u_z)/(\nu/D)$
W	width of solution domain

Greek

β	isobaric coefficient of thermal expansion
θ	dimensionless temperature, $(T-T_\infty)/(T_{cylinder}-T_\infty)$
μ	dynamic viscosity of the fluid
ν	kinematic viscosity of the fluid
ξ	curvature parameter, $(4L/D)(Gr_L/4)^{-1/4}$
ρ	density of the fluid

INTRODUCTION

Laminar natural convection heat transfer from the vertical surface of a cylinder is a classical subject, which has been studied extensively. When the radius of curvature of a vertical cylinder is large (i.e. the height-to-diameter aspect ratio is small), the surface of the cylinder can be approximated as a flat plate because geometric effects of the curvature are small enough to be ignored. However, when the radius of curvature of a vertical cylinder is small (i.e. the height-to-diameter ratio is large), the heat transfer deviates from the flat-plate approximation because geometric effects become important. Many investigators have studied the curvature limits for which the flat-plate model can be applied to estimate Nusselt numbers for vertical cylinders. Furthermore, these investigators have presented Nusselt number correlations for isothermal vertical cylinders.

In most heat transfer textbooks, including but not limited to Incropera, et al. [1, 2], Holman [3], Burmeister [4], and Gebhart, et al. [5], the accepted limit for which the flat-plate solution can be used to approximate average Nusselt numbers for vertical cylinders (Pr = 0.72) within 5% error is

$$\frac{D}{L} < \frac{35}{Gr_L^{0.25}} \quad (1)$$

where D is the diameter of the cylinder, L is the height of the cylinder, and Gr_L is the Grashof number based on the height of the cylinder. This limit was derived by Sparrow and Gregg [6] in 1956 using a perturbation technique for solving the heat transfer and fluid flow adjacent to an isothermal vertical cylinder. They assumed the boundary layer thickness at the leading edge to be zero and they made use of the boundary layer approximation (all pressure gradients are zero and streamwise second derivatives are neglected) and Boussinesq approximation (density difference are small). In addition, Nusselt numbers for vertical cylinders (Pr = 0.72 and 1; $0 < \xi < 1$) are presented as a truncated series solution and plotted. The curvature parameter ξ arose from a coordinate transformation done by [6] and is defined as

$$\xi = \frac{4L}{D}\left(\frac{Gr_L}{4}\right)^{-1/4} \quad (2)$$

Le Fevre and Ede [7,8] solved the governing equations using the same assumptions as [6], but instead used an integral method to obtain the following correlation for vertical cylinder average Nusselt numbers.

$$Nu_L = \frac{4}{3}\left[\frac{7Gr_L Pr^2}{5(20+21Pr)}\right]^{1/4} + \frac{4(272+315Pr)L}{35(64+63Pr)D} \quad (3)$$

In this equation, Nu_L is the average Nusselt number and Pr is the Prandtl number.

Cebeci [9] extended the work of [6] by numerically solving the governing equations using the boundary-layer approximation for a wider range of Prandtl numbers and curvature parameters ($0.01 \leq Pr \leq 100$ and $0 < \xi < 5$). The results of Cebeci for the average Nusselt number for an isothermal vertical cylinder fpr Pr = 0.72 have been correlated in Popiel [10] with a range of deviation from -0.34% - 0.66%

$$\frac{Nu_L}{Nu_{L,fp}} = 1 + 0.3\left[32^{0.5} Gr_L^{-0.25} \frac{L}{D}\right]^{0.909} \quad (4)$$

In this equation, $Nu_{L,fp}$ is the average Nusselt number for the isothermal flat plate. Typically, the value for $Nu_{L,fp}$ is taken from the Churchill and Chu [11] correlations for natural convection from a vertical flat plate.

$$Nu_{L,fp} = 0.68 + \frac{0.670 Ra_L^{1/4}}{[1+(0.492/Pr)^{9/16}]^{4/9}} \quad (5)$$

In this equation, Ra_L is the Rayleigh number based on the height of the cylinder.

Minkowycz and Sparrow [12] reexamined the accuracy of [6] by investigating the impact of different levels of truncation in the series solution. Their findings indicate good agreement with [6] with a maximum deviation of 4% between the average Nusselt number solutions.

Later, Lee et al. [13] solved the boundary layer equations for non-uniform wall temperature using the similarity solution method. Their work extends that of Fujii and Uehara [14], except that unlike the authors of [14] who present information for local Nusselt numbers only, the authors of [13] present correlations for both the local and average Nusselt numbers. The average Nusselt number correlation in [13] for $0.1 \leq Pr \leq 100$ when the wall temperature is uniform is

$$ln\left[Nu_L\left(\frac{Gr_L}{4}\right)^{-\frac{1}{4}}\right] = F(\xi) + \left\{ln\left[Nu_{L,fp}\left(\frac{Gr_L}{4}^{-\frac{1}{4}}\right) + 2.92629\right]\right\} exp(-G\xi^{1/2}) \quad (6)$$

and F and G are functions such that

$$F(\xi) = -2.92620 + 1.66850\xi^{1/2} - 0.21909\xi + 0.011308\xi^{3/2} \quad (7)$$

and

$$G = 0.29369 + 0.32635 Pr^{-0.19305} \quad (8)$$

with $\mathrm{Nu}_{L,fp}$ being defined as

$$Nu_{L,fp}\left(\frac{Gr_L}{4}\right)^{-1/4} = (2Pr)^{1/2}[2.5(1+2Pr^{1/2}+2Pr)]^{-1/4} \quad (9)$$

Although much classical work on the natural convection heat transfer from isothermal vertical cylinders has been reported, there has been recent interest in the subject as seen by a contemporary review article in 2008 on the subject by Popiel [10] and several investigators using either experimental means [15, 16] or older analytical and numerical techniques [17].

Popiel et al. [16] conducted an experimental study on natural convection from an isothermal vertical cylinder. In addition to the experiments, the investigators in [16], using the data reported [9], propose a new limit for which the flat plate solution can be used to approximate the average Nusselt numbers with 3% error

$$Gr_L^{0.25}\frac{D}{L} \leq a + \frac{b}{Pr^{0.5}} + \frac{c}{Pr^2} \quad (10)$$

where a = 11.474, b = 48.92, and c =-0.006085. Furthermore, experiments were conducted on an isothermal vertical cylinder with an insulated top situated on an insulated surface for Pr = 0.71, $1.5 \times 10^8 < \mathrm{Ra}_L < 1.1 \times 10^9$, and 0 < L/D < 60. The results of this study were correlated into the following equation

$$Nu_L \leq A Ra_L^n \quad (11)$$

where

$$A = 0.519 + 0.03454\frac{L}{D} + 0.0008772\left(\frac{L}{D}\right)^2 + 8.855 \times 10^{-6}\left(\frac{L}{D}\right)^3 \quad (12)$$

and

$$n = 0.25 - 0.00253\frac{L}{D} + 1.152 \times 10^{-5}\left(\frac{L}{D}\right)^2 \quad (13)$$

Their results agreed fairly well with [9] for the higher Rayleigh numbers which were studied.

High-quality natural convection heat transfer experiments that correctly interrogate heated shapes in air are inherently difficult to perform. Much analytical and numerical work is incomplete due to the practices of 1) neglecting the streamwise second derivative in the Navier-Stokes equation (i.e., boundary-layer approximation) and 2) using boundary conditions that are not representative of the space surrounding real objects. Previous work typically places the boundary at the top of the cylinder instead of considering the effect of the resulting plume on the boundary layer of the vertical surface.

The goal of this work is to perform numerical experiments which take into account the streamwise second derivatives in the governing equations and allow for full plume growth to determine average Nusselt numbers for isothermal vertical cylinders ($10^3 < \mathrm{Ra}_L < 10^9$, 0.5 < L/D < 10, and Pr = 0.7) situated on an adiabatic surface in a quiescent ambient environment which will allow for plume growth. In addition, the validity of Eqs. (1) and (10) for determining the range at which the flat-plate solution may be used as an approximation for a vertical cylinder will be investigated.

PROBLEM FORMULATION

Physical Model and Solution Domain

Consider a vertical cylinder with isothermal walls and an adiabatic top of diameter D and height L situated on an adiabatic surface in a quiescent, constant-temperature ambient environment. The top is taken to be adiabatic in order to investigate the accuracy of the classical side-wall solutions; although, solutions were ran with an isothermal top and those results were identical to the results for an adiabatic top. Due to both geometric and thermal axisymmetry, this problem may be modeled as two-dimensional. The solution domain is presented in Fig. 1.

In Fig. 1 r and z are the radial and axial coordinates, respectively. Furthermore, W is the width of the solution domain which is set to 5D and H is the height of the solution domain which is equal to (24D + L). The aspect ratio of the cylinder AR = D/L is varied parametrically, $0.5 \leq \mathrm{AR} \leq 10$.

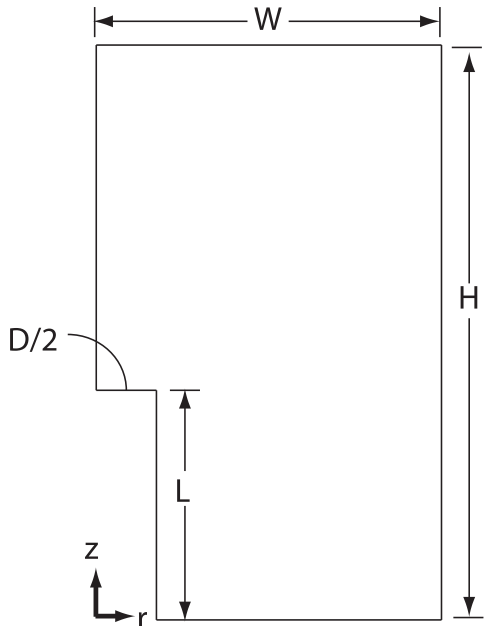

FIGURE 1. SCHEMATIC DIAGRAM OF THE SOLUTION DOMAIN.

Governing Equations

The subsequent dimensionless variables are used in writing the governing equations

$$R = \frac{r}{L}, \quad Z = \frac{z}{L}, \quad U_R = \frac{u_r}{\nu/L}, \quad U_Z = \frac{u_z}{\nu/L}$$
$$\theta = \frac{T - T_\infty}{T_{cylinder} - T_\infty}, \quad P = \frac{p - p_\infty}{\rho(\nu/L)^2} \tag{14}$$

and

$$Gr_L = \frac{g\beta(T_{cylinder} - T_\infty)}{\nu^2}, \quad Pr = \frac{c_p\mu}{k} \tag{15}$$

Here, r and z are the radial and axial coordinates respectively, u_r and u_z are the radial and axial velocity components, ν is the kinematic viscosity, T is the temperature, $T_{cylinder}$ is the temperature at the wall of the cylinder, T_∞ is the ambient temperature far from the cylinder, p is the local pressure, p_∞ is the freestream pressure, g is gravity, β is the coefficient of thermal expansion, c_p is the specific heat at constant pressure, μ is the dynamic viscosity and k is the thermal conductivity. All thermal properties are assumed to be constant.

The governing equations for axisymmetric, laminar, incompressible, natural convection flow are

Conservation of Mass

$$\frac{1}{R}\frac{\partial(RU_R)}{\partial R} + \frac{\partial(U_Z)}{\partial Z} = 0 \tag{16}$$

Conservation of Momentum in the Z-direction

$$U_R\frac{\partial U_Z}{\partial R} + U_Z\frac{\partial U_Z}{\partial Z} = -\frac{\partial P}{\partial Z} + \frac{1}{R}\frac{\partial}{\partial R}R\frac{\partial U_Z}{\partial R} + \frac{\partial^2 U_Z}{\partial Z^2} + Gr_L\theta \tag{17}$$

Conservation of Momentum in the R-direction

$$U_R\frac{\partial U_R}{\partial R} + U_Z\frac{\partial U_R}{\partial Z} = -\frac{\partial P}{\partial R} + \frac{1}{R}\frac{\partial}{\partial R}R\frac{\partial U_R}{\partial R} + \frac{\partial^2 U_R}{\partial Z^2} - \frac{U_R}{R^2} \tag{18}$$

Conservation of Energy

$$U_R\frac{\partial \theta}{\partial R} + U_Z\frac{\partial \theta}{\partial Z} = \frac{1}{Pr}\left[\frac{1}{R}\frac{\partial}{\partial R}R\frac{\partial \theta}{\partial R} + \frac{\partial^2 \theta}{\partial Z^2}\right] \tag{19}$$

The Boussinesq approximation can be employed here due to negligible density differences. The viscous dissipation and work terms can be neglected in the energy equation because of the small velocities encountered in natural convection flow.

Boundary Conditions

The temperature at the vertical surface of the cylinder is $T_{cylinder}$ and the no-slip condition is applied. The boundary conditions at the surface of the cylinder in dimensionless form are

$$U_R = U_Z = 0 \ \ and \ \ \theta = 1 \tag{20}$$

On the top surface of the cylinder and the bottom surface of the fluid domain, adiabatic and no-slip boundary conditions are applied such that

$$U_R = U_Z = 0 \ \ and \ \ \frac{\partial \theta}{\partial Z} = 0 \tag{21}$$

Along the axis of symmetry (R = 0) the boundary conditions are

$$U_R = \frac{\partial U_Z}{\partial R} = \frac{\partial \theta}{\partial R} = 0 \qquad (22)$$

Relatively weak boundary conditions (the so-called opening condition in ANSYS CFX) are placed at the far-field boundaries at the top and side of the solution domain. The conditions allow the flow to either entrain into the domain or flow out. Specified at these boundaries are the pressure and the temperature of the fluid if entering into the domain.

At the top of the solution domain

$$P = 0 \;\; and \;\; \theta = 0 \;\; if \;\; U_Z < 0 \qquad (23)$$

Along the side of the solution domain

$$P = 0 \;\; and \;\; \theta = 0 \;\; if \;\; U_R < 0 \qquad (24)$$

SOLUTION

ANSYS CFX 12.0, a finite-volume-based computational fluid dynamics solver, was used to perform the numerical experiments. Unlike the classical methods of using the integral method, solving for the boundary layer equations, and/or pertubation techniques, ANSYS CFX 12.0 solves for the full conservation of mass, momentum, and energy equations. Furthermore, in the numerical approach here, solution domain boundaries are extended further out minimizing boundary condition assumptions in the area of the flow (i.e. the plume at the top of the cylinder is allowed to grow, whereas in the classicals solutions, the boundary is cut-off at the top of the cylinder).

The number of nodes used was 210,000. Mesh independence was established by multiplying the number of nodes by two. The average Nusselt numbers of the two meshes varied by less than 0.3%.

In addition, the height and width of the solution domain was investigated. The boundaries of the solution domain were placed far enough away as to not affect the solution of the area of interest, in this case, the heat transfer at the cylinder. Several domain widths and heights were tested.

RESULTS AND DISCUSSION

Figures 2-7 have been prepared to show the average Nusselt numbers versus Rayleigh number for several different aspect ratios. The current numerical experiments (Present) are compared with previous work by LeFevre and Ede [7, 8] - Eq. (3), Cebeci [9] - Eq. (4), Lee et al. [13] - Eqs. (6-9), Popiel [10] - Eqs. (10-13), and the isothermal laminar vertical flat plate correlation from Churchill and Chu [11] - Eq. (5). The results of Sparrow and Gregg [6] and Minkowycz and Sparrow [12] are in good agreement with the work of Cebeci [9] so they are not

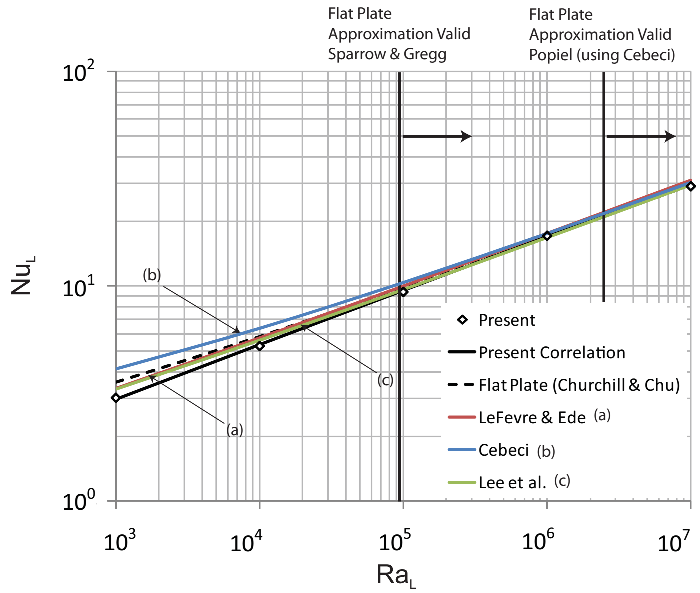

FIGURE 2. AVERAGE NUSSELT NUMBER VERSUS RAYLEIGH NUMBER FOR AR = 0.5.

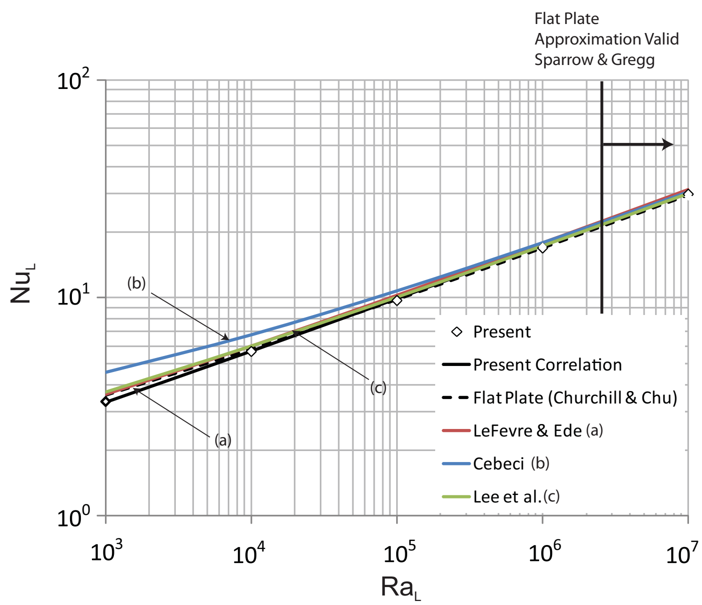

FIGURE 3. AVERAGE NUSSELT NUMBER VERSUS RAYLEIGH NUMBER FOR AR = 1.

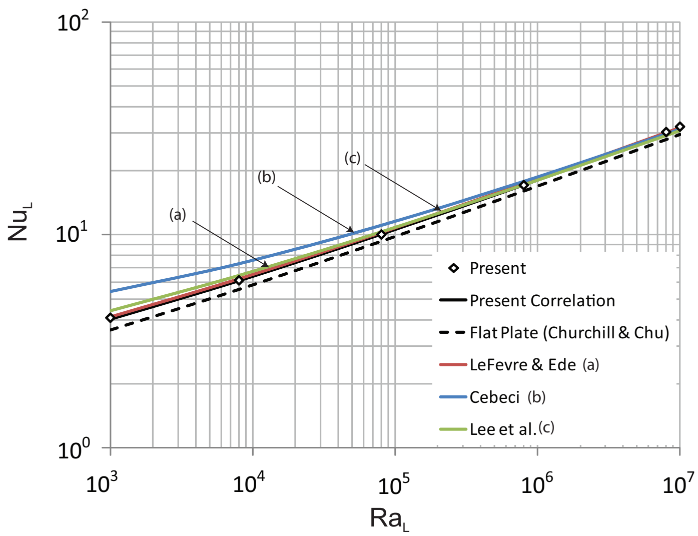

FIGURE 4. AVERAGE NUSSELT NUMBER VERSUS RAYLEIGH NUMBER FOR AR = 2.

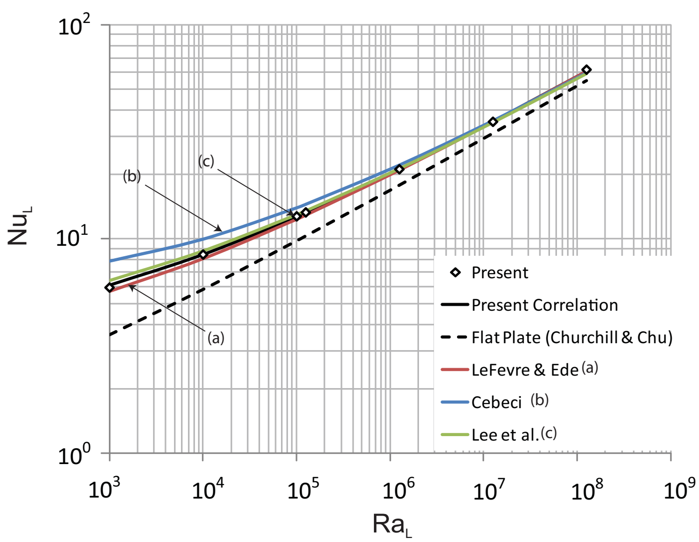

FIGURE 5. AVERAGE NUSSELT NUMBER VERSUS RAYLEIGH NUMBER FOR AR = 5.

plotted here. Furthermore, the present data has been correlated into an equation for Pr = 0.7 and plotted in the figures. The resulting correlation was developed using the MATLAB surface fitting tool using a non-linear least squares method with a LAR robust algorithm. The R-squared value of 0.9999.

$$Nu_L = -0.4192 + 0.541 Ra_L^{-1/4} + 0.6897 \left[\frac{L}{D}\right] \qquad (25)$$

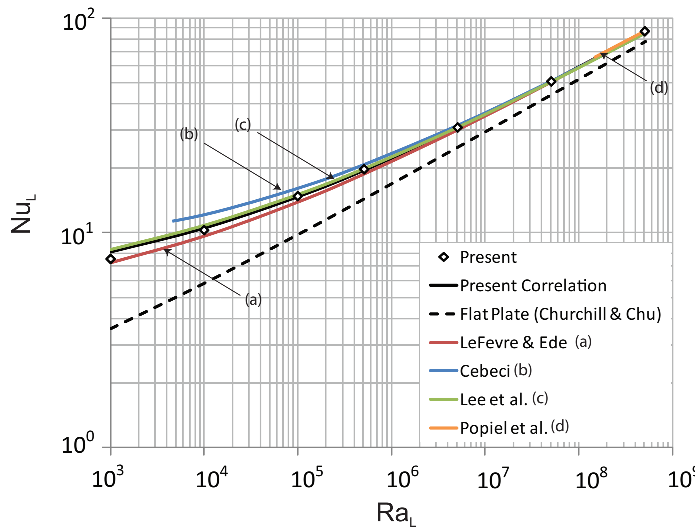

FIGURE 6. AVERAGE NUSSELT NUMBER VERSUS RAYLEIGH NUMBER FOR AR = 8.

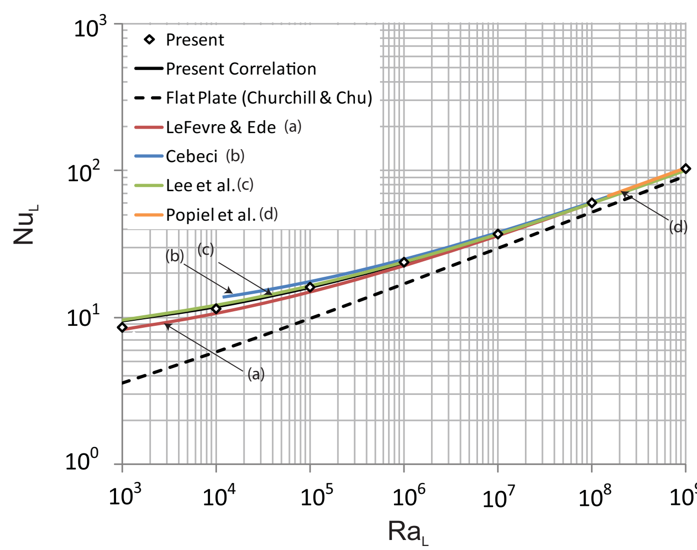

FIGURE 7. AVERAGE NUSSELT NUMBER VERSUS RAYLEIGH NUMBER FOR AR = 10.

The applicability limits of the isothermal vertical flat-plate solution as an approximation of the average heat transfer coefficient for an isothermal vertical cylinder are shown in Figs. 2 and 3 (for Figs. 4 - 7 the limits are located at Ra_L greater than those of interest). These figures include the range proposed by Sparrow and Gregg [6] (Eq. 1) and the more conservative estimate provided by Popiel using the data of Cebeci [9, 10] (Eq. 10).

As the Rayleigh number increases, all solutions asymptotically approach the flat-plate solution. As expected, lower values of the aspect ratio approach the flat-plate solution faster than higher values of the aspect ratio.

In Fig. 2, the present solution Eq. 25, at $\mathrm{Ra}_L = 10^3$, deviates from the flat-plate solution by 15%, from Cebeci by 26%, and from LeFevre and Ede and Lee et al. by about 9%. These differences are significant. As the Rayleigh number increases, the solution by LeFevre and Ede and Lee et. al converge to the present solution faster than the Cebeci solution. The present data begins to deviate from the flat-plate solution for Rayleigh numbers less than 10^5, suggesting that for this particular aspect ratio (AR = 0.5), the Sparrow and Gregg limit is acceptable.

Next, attention will be turned to Fig. 3. Here, the present data, along with the data of LeFevre and Ede, Lee et al., match very closely to that of the flat plate solution. The maximum deviation of these data sets is 6% from that of the flat plate at $\mathrm{Ra}_L = 10^3$. This result shows that the Sparrow and Gregg limit is much too conservative in predicting the flat-plate limit for this aspect ratio. A limit placed at $\mathrm{Ra}_L \approx 2500$ for this case would be more accurate for predicting the point at which the cylinder Nusselt numbers deviate from the flat-plate by more than 5%. Furthermore, the present data differs from Cebeci by 26% for the lowest Rayleigh number.

In Figs. 4 - 7, the present data differs from that of the flat-plate data by more than 5% for all Rayleigh numbers. For these cases, the Sparrow and Gregg limit would be off of the graph at $\mathrm{Ra}_L = 3.8 \times 10^8$ for AR = 2 and $\mathrm{Ra}_L > 1.5 \times 10^{10}$ (turbulent region) for AR = 5, 8, and 10. Again, it is interesting to note that the Cebeci data differs significantly from the present solution and that of LeFevre and Ede and Lee et al., as much as 25% in Figs. 4 and 5, and 15% in Figs. 6 and 7. Cebeci only carried out his work for $0 < \xi < 5$, and the lower Rayleigh numbers for AR = 8 and 10 in Figs. 6 and 7 did not fall into this range, hence the non-inclusion of this data on the chart for the lower Rayleigh numbers.

It is of particular interest to note that in many heat transfer textbooks, including [1–3], after determining whether curvature effects are important using Eq. 1, the reader is directed to use the results of [6], [9], and/or [12],which are the results from Sparrow and Minkowycz and Cebeci. From the graphs, the Cebeci data approaches that of the other solutions as the aspect ratio increases as well as when the Rayleigh number increases; however, for lower values of the aspect ratio and Rayleigh number, the Cebeci data differs from the present results by as much as 26%.

CONCLUDING REMARKS

In the present study, numerical experiments have been performed to interrogate the average Nusselt numbers for isothermal vertical cylinders situated on an adiabatic surface in a quiescent ambient environment for Pr = 0.7, $10^3 < \mathrm{Ra}_L < 10^9$, and $0.5 <$ L/D < 10.

The resulting data are not always in agreement with the commonly used correlations of Cebeci. Instead, the resulting data are in better agreement with the correlations of LeFevre and Ede, which are implied to be less accurate because they were derived using an integral method. Further investigation, such as running a numerical experiment with the boundary conditions of previous investigators, is needed to determine the cause of this discrepancy. In addition, more numerical experiments with a wider range of parameters are needed.

REFERENCES

[1] Incropera, F. P., Dewitt, D. P., Bergman, T. L., and Lavine, A. S., 2007. *Introduction to Heat Transfer 5th Ed.* John Wiley & Sons, Inc., Hoboken, NJ.

[2] Incropera, F. P., Dewitt, D. P., Bergman, T. L., and Lavine, A. S., 2007. *Fundamentals of Heat and Mass Transf 6th Ed.* John Wiley & Sons, Inc., Hoboken, NJ.

[3] Holman, J. P., 2010. *Heat Transfer 10th Ed.* Mc-Graw-Hill Companies, Inc., New York, NY.

[4] Burmeister, L., 1993. *Convective Heat Transfer 2nd Ed.* John Wiley & Sons, In, New York, NY.

[5] Gebhart, B., Jaluria, Y., Mahajan, R. L., and Sammakia, B., 1988. *Buoyancy-Induced Flows and Transport: Reference Edition*. Hemisphere Publishing Company, New York, NY.

[6] Sparrow, E. M., and Gregg, J. L., 1956. "Laminar-free-convection heat transfer from the outer surface of a vertical circular cylinder". *Transactions of the ASME,* ***78***, pp. 1823–1829.

[7] LeFevre, E. J., and Ede, A. J., 1956. "Laminar free convection from the outer surface of a vertical cylinder". In Proceedings of the 9th International Congress on Applied Mechanics, pp. 175–183.

[8] Ede, A. J., 1967. *Advances in Heat Transfer*. ch. Advances in Free Convection, pp. 1–64.

[9] Cebeci, T., 1974. "Laminar-free-convective-heat transfer from the outer surface of a vertical circular cylinder". In Proceedings of the 5th International Heat Transfer Conference, Tokyo, pp. 1–64.

[10] Popiel, C. O., 2008. "Free convection heat transfer from vertical slender cylinders: A review". *Heat Transfer Engineering,* ***29***, pp. 521–536.

[11] Churchill, S. W., and Chu, H. H. S., 1975. "Correlating equations for laminar and turbulent free convection from a vertical plate". *International Journal of Heat and Mass Transfer,* ***18***, pp. 1323–1329.

[12] Minkowycz, W. J., and Sparrow, E. M., 1974. "Local non-similar solutions for natural convection on a vertical cylinder". *Journal of Heat Transfer,* ***96***, pp. 178–183.

[13] Lee, H. R., Chen, T. S., and Armaly, B. F., 1988. "Natural convection along slender vertical cylinders with variable surface temperature". *Journal of Heat Transfer,* ***110***, pp. 103–108.

[14] Fujii, T., and Uehara, H., 1970. "Laminar natural-

convective heat transfer from the outside of a vertical cylinder". *International Journal of Heat and Mass Transfer,* ***13***, pp. 607–615.

[15] Kimura, F., Tachibana, T., Kitamura, K., and Hosokawa, T., 2004. "Fluid flow and heat transfer of natural convection around heated vertical cylinders (effect of cylinder diameter)". *JSME International Journal Series B,* ***47***, pp. 159–161.

[16] Popiel, C. O., Wojtkowiak, J., and Bober, K., 2007. "Laminar free convective heat transfer from isothermal vertical slender cylinders". *Experimental Thermal and Fluid Science,* ***32***, pp. 607–613.

[17] Gori, F., Serrano, M. G., and Wang, Y., 2006. "Natural convection along a vertical thin cylinder with uniform and constant wall heat flux". *International Journal of Thermophysics,* ***27***, pp. 1527–1538.